Hindawi
Science and Technology of Nuclear Installations
Volume 2017, Article ID 9152580, 5 pages
https://doi.org/10.1155/2017/9152580

Research Article

Analyses of the TIARA 43 MeV Proton Benchmark Shielding Experiments Using the ARES Transport Code

Bin Zhang, Liang Zhang, and Yixue Chen

North China Electric Power University, No. 2 Beinong Road, Changping District, Beijing 102206, China

Correspondence should be addressed to Bin Zhang; zhangbin@ncepu.edu.cn

Received 29 April 2017; Revised 16 June 2017; Accepted 27 June 2017; Published 24 July 2017

Academic Editor: Rafael Miró

ARES is a multidimensional parallel discrete ordinates particle transport code with arbitrary order anisotropic scattering. It can be applied to a wide variety of radiation shielding calculations and reactor physics analysis. To validate the applicability of the code to accelerator shielding problems, ARES is adopted to simulate a series of accelerator shielding experiments for 43 MeV proton-^{7}Li quasi-monoenergetic neutrons, which is performed at Takasaki Ion Accelerator for Advanced Radiation Application. These experiments on iron and concrete were analyzed using the ARES code with FENDL/MG-3.0 multigroup libraries and compared to direct measurements from the BC501A detector. The simulations show good agreement with the experimental data. The ratios of calculated values to experimental data for integrated neutron flux at peak and continuum energy regions are within 64% and 25% discrepancy for the concrete and iron experiments, respectively. The results demonstrate the accuracy and efficiency of ARES code for accelerator shielding calculation.

1. Introduction

Validation is an essential part of software quality assurance to ensure that the solutions obtained from the code match reality sufficiently well. Therefore, validation requires comparison of computed results with experimentally measured data. For reliable accelerator shielding calculations, it is necessary to validate the transport code through analyses of shielding experiments. This paper reports on the validation exercise based on the Takasaki Ion Accelerator for Advanced Radiation Application (TIARA) [1] at Japan Atomic Energy Research Institute (JAERI), one of a set of international benchmark experiments for accelerator shielding.

Shielding analyses for the TIARA pose significant computational challenges, including highly anisotropic high energy sources and a combination of deep penetration shielding and unshielded beamline. The experiments on iron and concrete were analyzed using the ARES code with FENDL/MG-3.0 [2] multigroup libraries to validate ARES performance.

The ARES methodologies are described and summarized in Section 2, and the shielding experiment details are presented in Section 3. Results and analysis are summarized in Section 4, and our concluding remarks are presented in Section 5.

2. ARES Methodology

ARES [3, 4] is a multidimensional parallel discrete ordinates neutral particle transport code that uses state-of-the-art methods to obtain accurate solutions to the Boltzmann transport equation. The ARES transport code system consists of seven main modules: DONTRAN1D, DONTRAN2D, DONTRAN3D, RAY2D, RAY3D, ARES_PRE, and ARES_POST. DONTRAN1D, DONTRAN2D, and DONTRAN3D are the DONTRAN series to solve one-, two-, and three-dimensional transport problems, respectively. RAY adopts the first collision source method to mitigate ray effects in two or three dimensions (RAY2D and RAY3D, resp.). ARES_PRE incorporates the geometry and material information of the calculated model and deals with the

quadrature sets and cross section message. Preliminary verification and validation for the ARES transport code system had been performed by experiment benchmarking and reference code.

ARES employs discrete ordinates method in discretizing angular variables and adopts spherical harmonic to expand scattering source. The angular variable is usually discretized by replacing angular integrals with quadrature sums. Ray effects are nonphysical anomalies that often appear in optically thin multidimensional discrete ordinates calculations because the solution propagates along a finite set of directions defined by the angular quadrature set. The first collision source method was used to eliminate or mitigate ray effects.

A variety of spatial differencing scheme options are available, including diamond difference (DD), with or without linear-zero flux fixup; theta weighted (TW); directional theta weighted (DTW); exponential directional weighted (EDW); and linear discontinuous finite element. The most general solution technique is source iteration, which is a simple and effective method for many classes of transport problems. However, for optically thick problems dominated by scattering, the source iteration method converges very slowly. Diffusion synthetic acceleration (DSA) has been shown to significantly decrease the iterations. ARES uses the Koch-Baker-Alcouffe parallel sweep algorithm to obtain high parallel efficiency.

The neutron transport calculation in the energy region between 20 and 100 MeV is the most crucial problem for accelerator shielding designs, because high energy neutrons have strong penetrability. The spatial differencing schemes are very important to accurately simulate neutron transport. The diamond difference method assumes a linear relationship between the directional flux at the cell center and cell boundaries and is simple and accurate for small mesh intervals. However, when the mesh interval is too large, measured along the discrete direction through the cell, the difference equations may yield negative fluxes, which cause oscillations in the iterative process and frequently cause negative scalar flux. The TW, DTW, and EDW variations on the DD method were developed to eliminate negative fluxes without significantly sacrificing computational cost or accuracy.

The balance equation can be obtained by integrating the angular discretized form of the transport equation over the mesh cell $(\Delta x, \Delta y, \Delta z)$:

$$\frac{\mu_m}{\Delta x}\left(\psi_{i,\text{out}} - \psi_{i,\text{in}}\right) + \frac{\eta_m}{\Delta y}\left(\psi_{j,\text{out}} - \psi_{j,\text{in}}\right) + \frac{\xi_m}{\Delta z}\left(\psi_{k,\text{out}} - \psi_{k,\text{in}}\right) + \Sigma_{t,i,j,k}\psi_A = q_A, \tag{1}$$

where $\vec{\Omega}_m = (\mu_m, \eta_m, \xi_m)$ is the discretized direction-of-flight variables, ψ_A is the cell average flux, and the entering and exiting angular fluxes are referred to using "in" and "out" subscripts. $\Sigma_{t,i,j,k}$ is the total cross section. q_A is known from previous source iteration and the entering angular fluxes are known from the boundary values. When using diamond difference scheme, the cell averaged angular flux can be calculated by

$$\psi_A = \frac{q_A V + 2\left|\mu_m\right| A\psi_{i,\text{in}} + 2\left|\eta_m\right| B\psi_{j,\text{in}} + 2\left|\xi_m\right| C\psi_{k,\text{in}}}{2\left|\mu_m\right| A + 2\left|\eta_m\right| B + 2\left|\xi_m\right| C + \Sigma_t V}, \tag{2}$$

where $A = \Delta y \Delta z$; $B = \Delta x \Delta z$; $C = \Delta x \Delta y$.

Ray effects are nonphysical oscillations in the scalar flux. They are caused by the inability of a quadrature set in discrete ordinates approximation to accurately integrate the angular flux. Ray effects may represent the most significant deficiency of the S_N method. The first collision source method [5] was employed to mitigate ray effects. The method analytically calculates the uncollided flux to obtain the first collision source term, which is then applied to calculate the collided flux using the standard S_N method. The total flux is composed of the uncollided and collided flux.

Thus, the first collision source method decomposes the flux $\psi^g(\vec{r}, \vec{\Omega})$ into uncollided components $\psi^g_{(u)}(\vec{r}, \vec{\Omega})$ and collided components $\psi^g_{(c)}(\vec{r}, \vec{\Omega})$:

$$\psi^g\left(\vec{r}, \vec{\Omega}\right) = \psi^g_{(u)}\left(\vec{r}, \vec{\Omega}\right) + \psi^g_{(c)}\left(\vec{r}, \vec{\Omega}\right) \tag{3}$$

and the transport equation is decomposed into

$$\begin{aligned}
&\vec{\Omega}\cdot\nabla\psi^g_{(u)}\left(\vec{r}, \vec{\Omega}\right) + \Sigma^g_t(\vec{r})\,\psi^g_{(u)}\left(\vec{r}, \vec{\Omega}\right) = q^g_e\left(\vec{r}, \vec{\Omega}\right),\\
&\vec{\Omega}\cdot\nabla\psi^g_{(c)}\left(\vec{r}, \vec{\Omega}\right) + \Sigma^g_t(\vec{r})\,\psi^g_{(c)}\left(\vec{r}, \vec{\Omega}\right) = \sum_{g'=1}^{G}\sum_{n=0}^{N}\frac{2n+1}{4\pi}\\
&\qquad\cdot\Sigma^{gg'}_{sn}(\vec{r})\sum_{k=-n}^{n}Y_{nk}\left(\vec{\Omega}\right)\phi^{g'(c)}_{nk}(\vec{r}) + q^{(u)}_s\left(\vec{r}, \vec{\Omega}\right),
\end{aligned} \tag{4}$$

where $q^g_e(\vec{r}, \vec{\Omega})$ is fixed source and $q^{(u)}_s(\vec{r}, \vec{\Omega})$ is the first collision source, which is calculated from uncollided flux moments. $\Sigma^{gg'}_{sn}$ is the Legendre moment of scattering cross section from group g' to group g, and Y_{nk} is spherical harmonics.

RAY employs ray tracing method to accelerate optical distance calculations, and the point source correction factor is introduced to improve the accuracy of calculation results. The RAY module within ARES has been verified elsewhere by a series of international benchmarks, such as Kobayashi benchmarks [6], and can effectively eliminate ray effects and obtain reasonable results.

3. Overview of Shielding Experiments

Figure 1 shows a cross sectional view of the TIARA facility with the experimental arrangement [7]. Quasi-monoenergetic source neutrons were generated by 43 MeV protons bombarding ^{7}Li targets. Neutrons produced in the forward angle reached the experiment room through a 10.9 cm diameter, 225 cm long iron collimator embedded in the concrete wall. A test shield of iron or concrete 10–150 cm

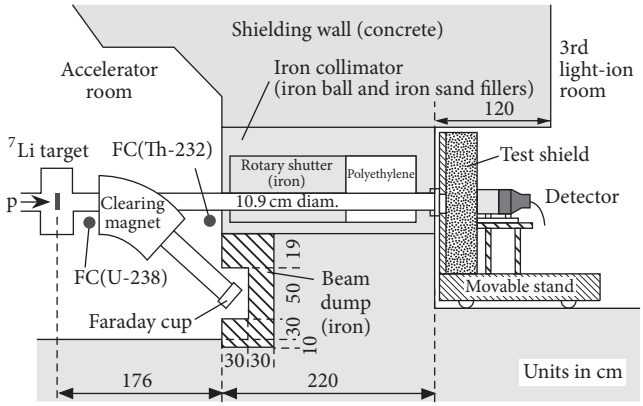

Figure 1: Experimental arrangement of shielding experiments.

thick was located at the end of the collimator with an additional iron shield. To measure the neutron energy spectra, a 12.7 cm diameter, 12.7 cm long BC501A liquid scintillation detector was placed behind the test shields. The density and the atomic composition of the concrete and iron shields are described in [8].

Source neutron spectra were obtained by TOF measurements. The peak energies of quasi-monoenergetic neutron sources were 40 MeV for 43 MeV protons, and the minimum neutron energy that could be measured with the TOF method was 7 MeV.

The experimental geometry was reproduced within the ARES discrete ordinates transport code with 69212 mesh. An isotropic neutron point source was set at the target position, with energy spectrum as shown in Figure 2 [9].

Fixed source calculations were performed in the P_5-S_{16} approximation, where P_5 corresponds to the order of the expansion in Legendre polynomials of the scattering cross section matrix, and S_{16} represents the order of the flux angular discretization. Level symmetric quadrature sets were applied to calculate the neutron flux. Diamond differencing with linear-zero flux fixup approximation was selected for the flux extrapolation model. In all the calculations the same numerical value ($1.0E-03$) for the point-wise flux convergence criterion was employed. Since the geometry included the narrow collimator, prior to the discrete ordinates calculation the first collision source was generated by the RAY3D code to remove the ray effects.

FENDL/MG-3.0 [10] multigroup libraries were used to simulate the TIARA benchmark shielding experiments. FENDL/MG-3.0 is a multigroup formatted library, intended for deterministic transport codes. The library contains multigroup cross section data in the 211n/42g Vitamin J+ energy structures (matching the 175n Vitamin J energy structure below 19.64 MeV) for multigroup transport codes.

4. Results and Discussion

We selected the BC501A detector measured neutron spectra at the beam axis behind 10, 20, and 40 cm thick iron and 25, 50, 100, and 150 cm thick concrete to validate ARES transport code. This paper compared ARES calculations and

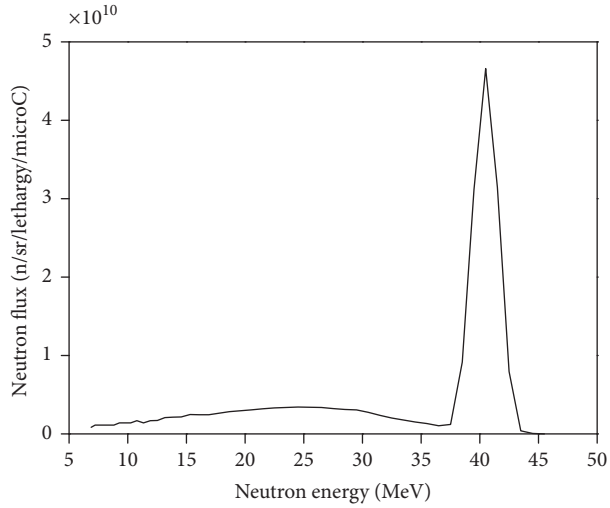

Figure 2: Source neutron spectra.

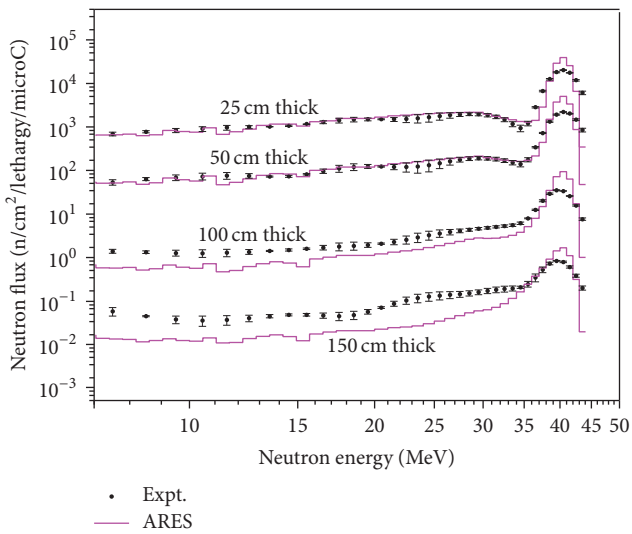

Figure 3: Measured and calculated neutron spectra of the concrete experiment.

measurements for neutron spectra above 7 MeV. Calculated values of the transmitted spectra were normalized by proton beam charge. Figures 3 and 4 show the measured and calculated neutron spectra on the beam axis for the concrete and iron experiment, respectively. Tables 1 and 2 summarize the ratios of the calculated to experimental values for the integrated neutron flux at peak and continuum energy regions. In addition, the MORSE Monte Carlo calculated results [1, 9] for concrete shielding and iron shielding are listed in Tables 1 and 2, respectively.

Figure 3 shows the measured and calculated neutron spectra of the concrete experiment for 43 MeV p-^{7}Li neutron sources. The ARES results show good agreement with the experimental data, but the agreement falls away with increasing assembly thickness. This underestimation is due to three factors:

Table 1: The ratio of calculation to measurement in peak and continuum regions for concrete shielding experiments.

Shield thickness (cm)	Peak region (35–45 MeV)				Continuum region (10–35 MeV)			
	Experimental (n/cm^2/s)	Calculated (n/cm^2/s)	C/E	C/E (MORSE)	Experimental (n/cm^2/s)	Calculated (n/cm^2/s)	C/E	C/E (MORSE)
25	2693.80	3303.74	1.23	1.07	1865.03	2020.65	1.08	1.11
50	300.45	423.04	1.41	1.09	156.29	166.03	1.06	1.42
100	5.03	8.27	1.64	1.19	3.34	1.83	0.55	1.70
150	0.12	0.17	1.42	1.26	0.11	0.04	0.37	2.11

Table 2: The ratio of calculation to measurement in peak and continuum regions for iron shielding experiments.

Shield thickness (cm)	Peak region (35–45 MeV)				Continuum region (10–35 MeV)			
	Experimental (n/cm^2/s)	Calculated (n/cm^2/s)	C/E	C/E (MORSE)	Experimental (n/cm^2/s)	Calculated (n/cm^2/s)	C/E	C/E (MORSE)
10	4205.53	5007.87	1.19	0.98	3539.32	3980.47	1.12	1.04
20	1022.81	1134.41	1.11	1.05	822.22	782.02	0.95	1.05
40	50.53	48.27	0.96	1.15	35.82	26.82	0.75	1.33

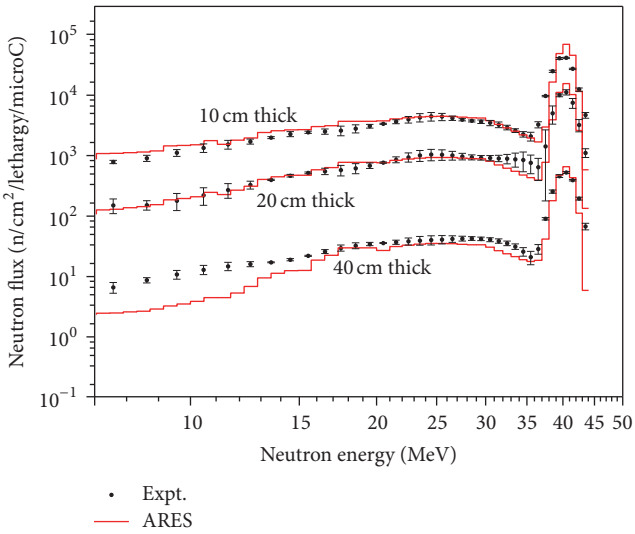

Figure 4: Measured and calculated neutron spectra of the iron experiment.

(1) Angular dependence of the differential scattering cross section is typically represented as a truncated Legendre series expansion. The accuracy of ARES calculations with $P5$ Legendre expansion for this problem worsens with increasing thickness, because the $P5$ Legendre expansion cannot present forward peaked angular distribution of secondary neutrons precisely for high energy neutrons.

(2) If the scattering cross section is highly anisotropic, the expansion may produce negative regions. Such anisotropy exists with light nuclei and nuclei at high energy. These negative regions may cause negative values in the discrete ordinates scattering source, which could greatly affect transport results [11].

(3) Discrete ordinates calculations are presumed to transport particles from cell to cell in the directions specified in the quadrature sets. However, diamond difference approximations introduce undamped lateral oscillations, resulting in severely nonphysical flux representations. Nonlinear fixups can prevent negativity but do not correct the underlying failure to properly propagate rays [12].

Table 1 compares the measured and calculated fluxes integrated into the continuum and the peak regions for 43 MeV p-^{7}Li neutron sources. The calculated spectra in the peak region agreed well with the measured spectra with 23%–64% discrepancy. In the continuum region the calculation provided smaller values than measured fluxes with increasing concrete thickness, but even in the worst case the ratio was 0.37.

Figure 5 depicts the 50 cm thick concrete shielding experiment model with neutron flux contours. The three largest energy group neutron fluxes have similar distributions.

Figure 4 shows the measured and calculated neutron spectra of the iron experiment for 43 MeV p-^{7}Li neutron sources. The ARES calculated results show good agreement to experimental data, except for neutron spectra below 17 MeV with 40 cm thickness iron shielding. ARES slightly underestimate spectra within 31~38 MeV when the iron thickness exceeds 20 cm. The main reason for this underestimation is the insufficiency of the Legendre expansion order for the scattering matrix in the multigroup libraries. The Legendre expansion order is usually 5 because of calculation constraints of the FENDL libraries. From 10 to 40 MeV intervals, the scattering cross section data of 56Fe is highly anisotropic, and truncation of a highly anisotropic scattering cross section may produce undesirable oscillations, producing regions where the cross section expansion becomes negative, with consequential effects on accuracy.

The calculations are in good agreement with measurements on the neutron beam axis for the 43-MeV p-^{7}Li neutron source with up to 25% discrepancy, as shown in Table 2. The calculated spectra in the peak region agreed

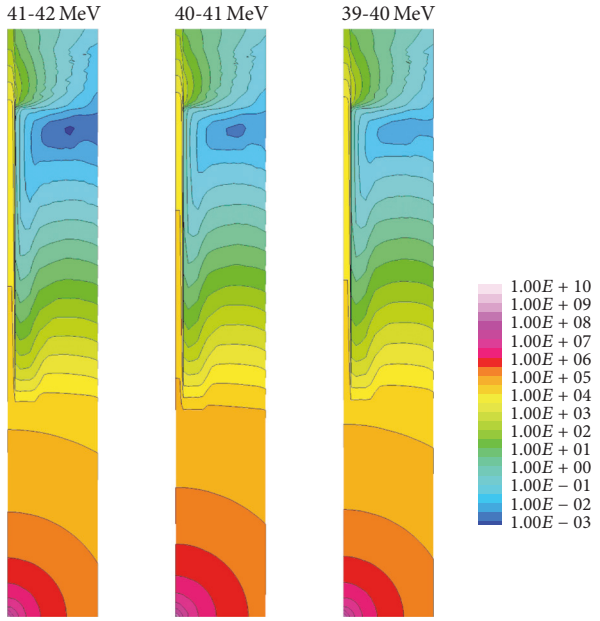

Figure 5: Neutron flux distribution of 50 cm thick concrete shielding experiment.

well with the measured spectra within 4–19% discrepancy. In the continuum region, the calculation provides smaller values than the measured fluxes with increasing iron thickness, but even in the 40 cm thick case the ratio is 0.75.

5. Conclusions

The accuracy of ARES calculations with FENDL/MG-3.0 libraries was investigated through analysis of iron and concrete shielding experiments for 43 MeV p-^{7}Li neutron sources at JAERI/TIARA. The ARES results show good agreement to experimental concrete shielding within 50 cm thickness and iron shielding within 20 cm thickness. As the shielding thickness increased, ARES underestimate the results. The calculated spectra in the peak region agreed well with the measured spectra, with up to 20% and 64% discrepancy for the iron and concrete experiments, respectively. In the continuum region the ARES calculation provided smaller values than the measured fluxes with increasing shielding thickness, with calculated/experiment rations 0.37–1.12.

In some energy regions, the underestimation can be improved by calculating with higher Legendre series expansion multigroup libraries and finer angular quadrature sets. Negative scattering source removal is an important research area in the process of ARES development. ARES is undergoing continuous development with many new features planned for implementation.

Conflicts of Interest

The authors declare that there are no conflicts of interest regarding the publication of this paper.

Acknowledgments

This work was supported by National Natural Science Foundation of China (11505059, 11575061) and the Fundamental Research Funds for the Central Universities (2016MS59).

References

[1] H. Nakashima, N. Nakao, S.-I. Tanaka et al., "Transmission through shields of quasi-monoenergetic neutrons generated by 43- and 68-MeV protons - II: Iron shielding experiment and analysis for investigating calculational method and cross-section data," *Nuclear Science and Engineering*, vol. 124, no. 2, pp. 243–257, 1996.

[2] C. Konno, K. Ochiai, S. Sato, and M. Ohta, "Analyses of iron and concrete shielding experiments at JAEA/TIARA with JENDL/HE-2007, ENDF/B-VII.1 and FENDL-3.0," *Fusion Engineering and Design*, vol. 98-99, pp. 2178–2181, 2015.

[3] Y. Chen, B. Zhang, L. Zhang, J. Zheng, Y. Zheng, and C. Liu, "ARES: A Parallel Discrete Ordinates Transport Code for Radiation Shielding Applications and Reactor Physics Analysis," *Science and Technology of Nuclear Installations*, vol. 2017, pp. 1–11, 2017.

[4] L. Zhang, B. Zhang, P. Zhang et al., "Verification of ARES transport code system with TAKEDA benchmarks," *Nuclear Instruments and Methods in Physics Research, Section A: Accelerators, Spectrometers, Detectors and Associated Equipment*, vol. 797, Article ID 57880, pp. 297–303, 2015.

[5] T. A. Wareing, J. E. Morel, and D. K. Parsons, *A First Collision Method for ATTILA, an Unstructured Tetrahedral Mesh Discrete Ordinates Code*, Los Alamos National Laboratory, USA, 1996.

[6] M. Chen, B. Zhang, and Y. Chen, "Verification for ray effects elimination module of radiation shielding code ARES by kobayashi benchmarks," in *Proceedings of the 22nd International Conference on Nuclear Engineering (ICONE '14)*, Prague, Czech Republic, July 2014.

[7] C. Konno, F. Maekawa, M. Wada, H. Nakashima, and K. Kosako, "DORT analysis of iron and concrete shielding experiments at JAERI/TIARA," in *Proceedings of JAERI Conference, JAERI-Conf-99-002*, pp. 164–169, 1999.

[8] Y. Nakane, K. Hayashi, Y. Sakamoto et al., *Neutron transmission benchmark problems for iron and concrete shields in low, intermediate and high energy proton accelerator facilities*, Japan Atomic Energy Research Institute, 1996.

[9] N. Nakao, H. Nakashima, T. Nakamura et al., "Transmission through shields of quasi-monoenergetic neutrons generated by 43- and 68-MeV protons - I: Concrete shielding experiment and calculation for practical application," *Nuclear Science and Engineering*, vol. 124, no. 2, pp. 228–242, 1996.

[10] R. A. Forresr, R. Capote, N. Otsuka et al., "FENDL-3 library summary documentation," *INDC(NDS)-0628, IAEA Nuclear Data Section*, 2012.

[11] J. A. Dahl, *Positive anisotropic scattering sources for discrete ordinate methods [Ph.D. thesis]*, University of Arizona, 1989.

[12] K. A. Mathews, "On the propagation of rays in discrete ordinates," *Nuclear Science and Engineering*, vol. 132, no. 2, pp. 155–180, 1999.